J. Min. Metall. Sect. B-Metall. 61 (2) (2025) 213 - 221

Journal of Mining and Metallurgy, Section B: Metallurgy

MICROSTRUCTURE AND HARDNESS OF Bi-MODIFIED MAGNESIUM AZ31 ALLOYS SUBJECTED TO SEVERE PLASTIC DEFORMATION

J. Yazdi, M.H. Farshidi [*], G.-R. Ebrahimi

Department of Materials Science and Engineering, Faculty of Engineering, Ferdowsi University of Mashhad, Azadi Square, Mashhad, Iran

(Received 17 May 2025; Accepted 25 August 2025)

Abstract

Magnesium alloys are known as attractive materials because of their low density and good thermal conductivity. However, compared to competing metallic materials such as aluminum alloys, magnesium alloys have lower strength. Among different methods introduced for strengthening metallic materials, severe plastic deformation is notable for its efficiency and relative simplicity. This study investigates the effect of bismuth content on the microstructure evolution and hardness of magnesium AZ31 alloy subjected to severe plastic deformation through equal channel angular pressing. For this purpose, AZ31 alloys with nominal bismuth contents of 0%, 1%, and 3% were processed by up to four passes of equal channel angular pressing at 300 °C. The microstructure evolution of these alloys was then examined using optical and scanning electron microscopy. The hardness of the specimens was measured using the Vickers method. Results show that bismuth-enriched second-phase particles are fragmented during severe plastic deformation. Additionally, increasing the bismuth content leads to more rapid grain refinement during severe plastic deformation due to the pinning effect of these second-phase particles on the grain boundaries. Faster hardening rates during severe plastic deformation were observed for the bismuth-containing AZ31 alloys. This effect is attributed to the more rapid grain refinement and the increase in the Hall-Petch coefficient resulting from the presence of fine bismuth-enriched particles.

Keywords: *Magnesium AZ31 alloy; Bismuth addition; Severe plastic deformation; Grain refinement; Hardness*

1. Introduction

Magnesium and its alloys have attractive characteristics like reasonable strength, good thermal conductivity, and low density. Therefore, they are attractive materials wherever the proportion of strength/density is essential, like the aircraft and the car manufacturing industries. Magnesium AZ alloys are the most commonly used because of their excellent castability, low costs, and relatively high strength. These alloys contain aluminum and zinc as the main alloying elements. In these alloys, the nominal weight percent concentrations of Al and Zn are presented in a code. For instance, the AZ31 contains 3 wt% of Al and 1 wt% of Zn. Aluminum increases the strength of AZ alloys by producing Mg17Al12 precipitates. Also, zinc is usually added to improve the strength of these alloys through the solid solution hardening. Adding Zn also increases the corrosion resistance of the alloy by removing different impurities like Fe and Ni from the matrix [1-3]. Besides Al and Zn, additions of other alloying elements like Sn, Bi, Gd, Y, and Ce to the magnesium alloys for improvement of their mechanical properties have been considered by different studies [2-10]. Among these elements, adding Bi can be more beneficial because of its considerable results and its reasonable costs. For more explanations, adding Bi causes the formation of Mg_3Bi_2 intermetallic particles composed of 85 wt% Bi and 15 wt% Mg. These particles elevate the strength of magnesium alloys, and they are thermally stable below 821 °C. Also, they enhance the creep resistance of these alloys by decreasing their grain growth rate [6-8, 11]. For more explanations, the presence of thermally stable particles prevents the rapid migration of grain boundaries at elevated temperatures, known as the Zener effect. Therefore, they decrease the grain growth rate [3, 6-10]. It is also notable that the workability of magnesium alloys at cold deformation regimes is limited because of the hexagonal close-pack crystal structure of magnesium having limited slip systems at low deformation temperatures. Therefore, these alloys are usually formed using warm/hot deformation regimes, whereas grain growth is a serious concern [2, 9, 12-13].

Corresponding author: farshidi@um.ac.ir

https://doi.org/10.2298/JMMB250517017Y

A well-known solution to improve the strength and ductility of the metallic materials is decreasing the grain size. For more explanations, the relation between the strength and the grain size of an alloy can be evaluated using the Hall-Petch equation as below [14]:

$$\sigma_{yl.} = \sigma_0 + KD^{-\frac{1}{2}} \quad (1)$$

Here, $\sigma_{yl.}$ is the yield strength, σ_0 is the frictional stress, K is the Hall-Petch slope, and D is the average grain size of the alloy. Except for the grain size, other microstructural features can affect the strength of the alloy and the parameters of Eq. 1. For instance, increasing the dislocation density can increase the frictional stress [14]. In addition, increasing the concentration of solute elements increases the Hall-Petch slope [15-16]. Also, the presence of second-phase particles can increase the Hall-Petch slope and the frictional strength [17-18].

Decreasing the grain size, usually called "grain refinement", can be achieved by applying a suitable thermomechanical process. For instance, the imposition of severe plastic deformation (SPD) is an outstanding method for the grain refinement of metallic materials. For this purpose, an equivalent plastic strain above 2 is imposed on the material [19-21]. For a better sense, this plastic strain equals a thickness reduction of 85% through flat rolling. The concept of severe plastic deformation in its modern form was developed by Segal et al. [22-23] during the 1970s. They have introduced a new process for SPD processing called equal channel angular pressing (ECAP). During previous decades, different studies have applied the concept of SPD for the grain refinement of magnesium alloys [13, 24-30]. For instance, the effects of SPD processing on the microstructure and mechanical properties of AZ31 have been investigated in different works. Results of these works have shown that the grain refinement and the increase of strength are considerable when using SPD at warm deformation temperatures (i.e., Tdef.~200 ºC or less). However, since the warm workability of magnesium alloys is limited, the low-temperature SPD processing of magnesium alloys causes the risk of fracture. On the other hand, the grain refinement and the hardening of the alloy become limited when using SPD at hot deformation temperature (i.e., Tdef. > 250 ºC) [13, 25-29]. For example, the decrease of the average grain size of the AZ31 alloy to 2-5 μm using four passes of ECAP at 200 ºC is frequently reported [13, 25-28]. However, when a similar process is applied at 275-300 ºC, the average grain size is 8-15 μm [25, 29]. Also, while the increase of the room temperature strength of the alloy to about 250 MPa through processing by four passes of ECAP at 200 ºC is reported [13], the room temperature strength of the alloy after four passes of ECAP at 250-300 ºC is in range of 150-180 MPa [27, 29]. These effects occur due to the rapid grain growth at hot deformation temperatures. One solution to prohibit the rapid grain growth is adding a thermally stable second-phase particle, likes the Mg_3Bi_2 mentioned above. However, no study has investigated the behavior of Bi-containing AZ magnesium alloys subjected to SPD processing at hot deformation temperatures.

This work aims to investigate the effect of Bi-addition on the microstructure and the hardening of the AZ31 magnesium alloy subjected to ECAP processing at a hot deformation regime. For this purpose, the AZ31 alloys with different bismuth contents are cast and processed through different passes of ECAP at 300 ºC. The microstructures of the processed specimens are observed by the optical and scanning electron microscopes. Also, the Vickers hardness measurement is applied to evaluate the hardening effect of the process.

2. Materials, Process and Experiments

Magnesium AZ31 alloys with 0, 1 wt%, and 3 wt% nominal Bi-content are cast and homogenized at 693 K for 16 h. The chemical compositions of the cast alloys are evaluated using optical emission spectrometry and presented in Table 1. After casting, 10 mm diameter rods are machined and subjected to ECAP processing at 300 ºC through route Bc. Fig. 1 shows the applied die set used for the ECAP processing. The used die has a channel angle of 90° with a corner radius of 2.5 mm. As shown before, the average strain imposed on a specimen by each pass of ECAP using this die is about 0.9. More details about the processing method have been presented before [31]. Hereafter, each specimen is called by a code showing its nominal composition and number of the imposed ECAP passes. For example, AZ31-1Bi-4 refers to the AZ31 alloy with 1wt% Bi-content subjected to 4 passes of ECAP.

The processed specimens are mechanically polished and then etched using PICRAL etchant. The microstructures of the specimens are observed by a

Table 1. *The chemical compositions of cast alloys in wt% evaluated using optical emission spectrometry*

Alloy	Al	Zn	Mn	Bi	Mg
AZ31-0Bi	2.5	0.7	0.18	-	Rem.
AZ31-1Bi	3.04	0.83	0.25	1.2	Rem.
AZ31-3Bi	2.81	0.74	0.27	3.1	Rem.

CC BY SA

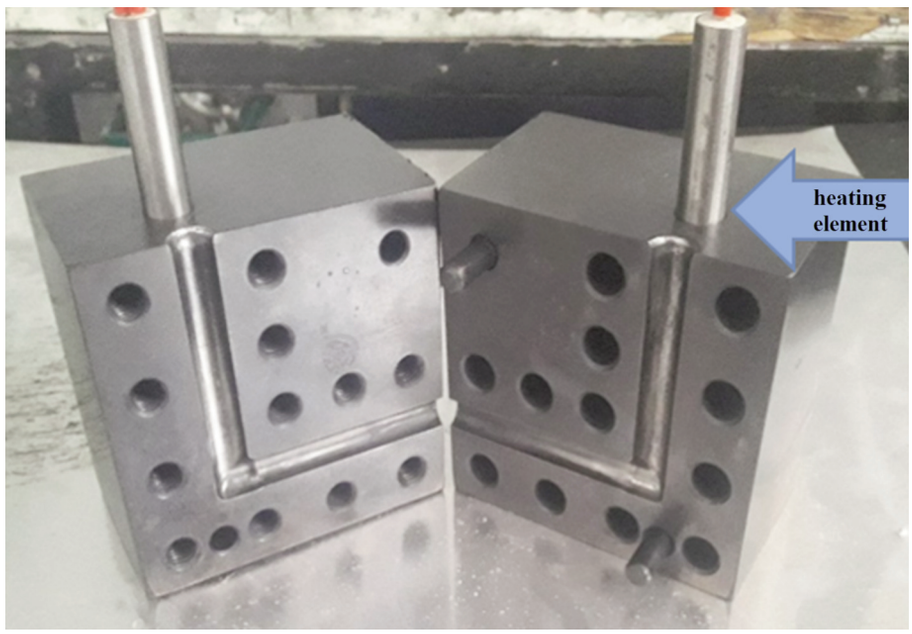

Figure 1. *The ECAP die used for the SPD processing*

BX-60M Olympus optical microscope (OM). The average grain size of each specimen is evaluated by MIP 4 image analyzing software according to ASTM E112 using figures captured by different magnifications. MIRA 3 TESCAN field emission scanning electron microscope (FESEM) is applied to study the second-phase particles inside the specimen's microstructure. Also, energy-dispersive X-ray spectroscopy (EDXS) is applied to evaluate the chemical compositions of second-phase particles of specimens. Also, the hardness of specimens is measured using the Vickers method (VHN) by the indentation load of 49 N.

3. Results and discussion

Fig. 2 compares the OM microstructures of the alloys before and after the imposition of the first pass of ECAP. As shown in Figs.2 (a) to (c), the microstructures of the unECAPed specimens are filled by coarse equiaxed grains. After one pass of ECAP, the microstructures of the alloys are transformed to a

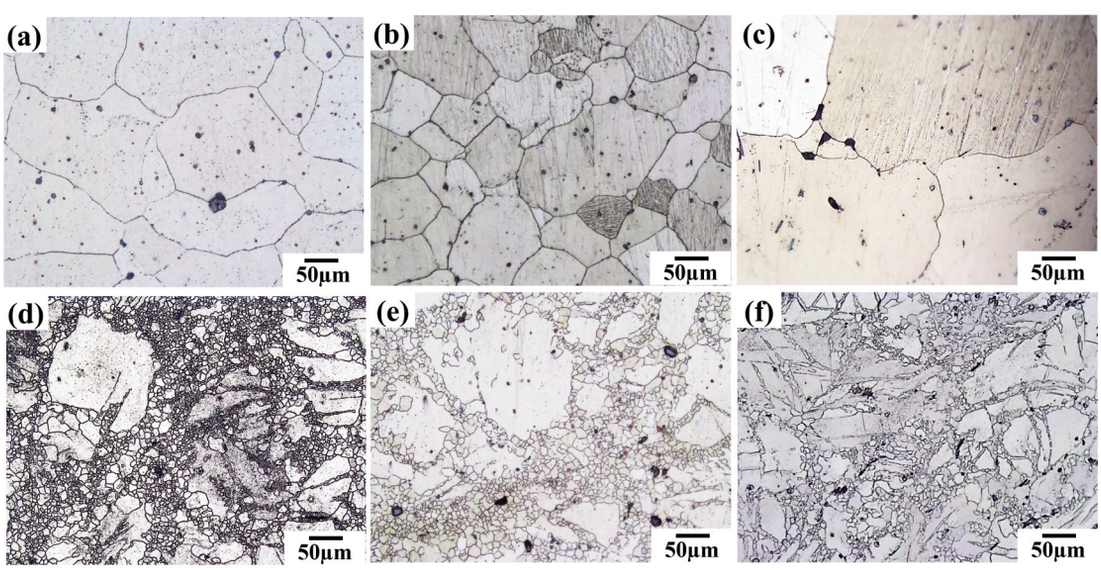

Figure 2. *OM microstructure of the: (a) AZ31-0Bi-0, (b) AZ31-1Bi-0, (c) AZ31-3Bi-0, (d) AZ31-0Bi-1, (e) AZ31-1Bi-1 and (f) AZ31-3Bi-1 specimens*

CC BY SA

necklace-shaped type, as shown in Figs. 2 (d) to (f). In these necklace-shaped microstructures, coarse grains are surrounded by refined grains sized a few micrometers. The incidence of these refined grains inside the microstructures of the alloys is attributed to the initiation of discontinuous dynamic recrystallizations (DDRX) in which the recrystallized grains nucleate near the grain boundaries of the initial coarse grains [19]. As shown in Figs. 3 (a) to (c), the progression of DDRX of alloys after the imposition of 2 passes is remarkable, whereas the bulk of alloys' microstructures are occupied by refined grains. After four passes of ECAP, almost whole of the alloy microstructures are occupied by the refined grains, as shown in Fig. 3 (d) to (f). This result indicates that the DDRX is nearly completed. Fig. 4 compares the average grain size of the alloys through processing by ECAP. As shown here, the grain size of AZ31-0Bi alloy after the imposition of four passes of ECAP is about 10 μm. This number is close to the results of previous works on this alloy at similar temperatures as mentioned above [25, 29]. Nonetheless, the average grain size of the AZ31-1Bi and AZ31-3Bi alloys after the imposition of four passes of ECAP is about 5 μm,

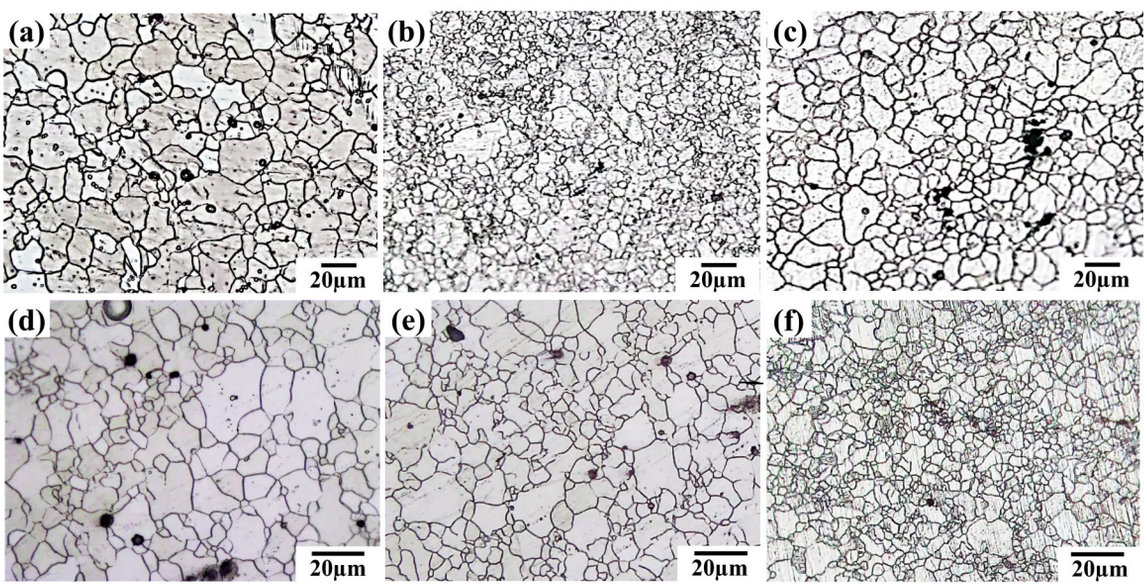

Figure 3. *OM microstructure of the: (a) AZ31-0Bi-2, (b) AZ31-1Bi-2, (c) AZ31-3Bi-2, (d) AZ31-0Bi-4, (e) AZ31-1Bi-4 and (f) AZ31-3Bi-4 specimens*

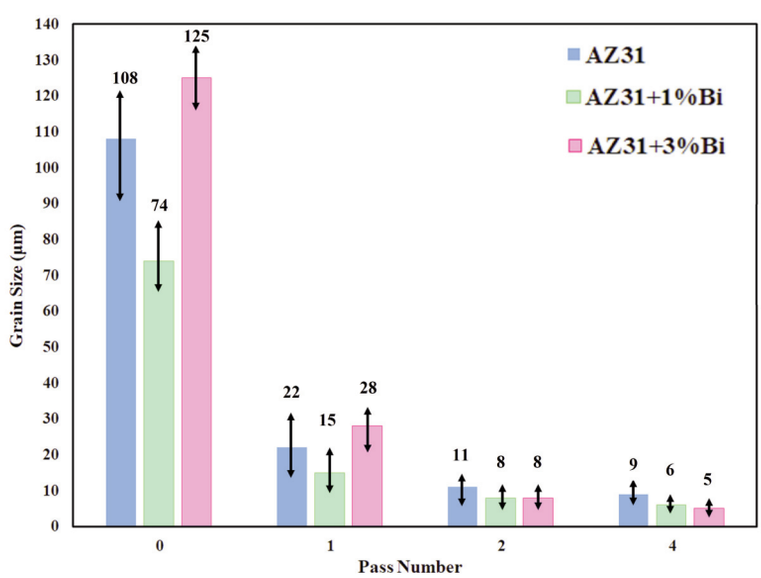

Figure 4. *Variation of the grain size of different alloys during ECAP processing*

considerably less than what is seen for the AZ31-0Bi alloy. These results indicate that the rate of grain refinement through the ECAP process is accelerated by adding Bi, as discussed later.

Fig. 5 compares the microstructures of the cast alloys observed by the FESEM. Results of EDXS for the composition of the second-phase particles shown in Fig. 5 are illustrated in Table 2. As shown here, adding Bi to the AZ31 magnesium alloy causes the formation of relatively coarse Bi-enriched particles inside the magnesium matrix. These Bi-enriched particles are white, and their chemical compositions are close to Mg_3Bi_2. Besides these Bi-enriched particles, grey-hue Al-enriched particles are formed due to the presence of Al. Fig. 6 shows the FESEM microstructure of the ECAP-processed alloys. As shown here, fine Bi-enriched particles inside the alloys can be seen after the ECAP processing. For instance, while the size of Bi-enriched particles before ECAP processing is about 10 μm, the size of these fine particles that appeared after the imposition of 4 passes of ECAP is less than 1 μm. As shown in Fig. 6 (e), this effect occurs by fragmentation of the Bi-enriched particles due to the imposition of an intense plastic deformation. Similarly, it is reported that coarse second-phase particles are fragmented during SPD due to a considerable stress concentration on these particles caused by the strain heterogeneity around these particles [32-35]. One can see that the fragmented Bi-enriched particles are often located on the boundaries of the refined grains that appeared during the ECAP process. This result occurs because of the pinning effect of these particles on the grain boundaries. This effect can explain the rapid grain refinement of Bi-containing AZ31 alloys mentioned above.

Table 2. *The chemical composition of particles in wt% evaluated using EDXS*

Particle No.	Al	Bi	Mg
1	0.3	72.7	26.9
2	68.4	7	24.5

Table 3 compares the effect of ECAP processing on the VHN of alloys. As shown here, the VHNs of the alloys increase by ECAP passes. According to the Hall-Petch relation, this effect is explained by the decrease in the grain size discussed above. However, one may question the effect of the Bi addition on the hardness increase. Fig. 7 compares the VHN of specimens versus the inverse square root of their grain size (D-0.5). As can be traced in Fig. 7, the increase of Bi-content increases the VHN in a constant grain size. This effect can be explained by the Bi-enriched particles formed due to adding Bi, as discussed above. As mentioned in explanations of Eq. 1, these particles increase the strength and the hardness by increasing the frictional stress (σ0). Regarding Eq. 1 and considering the VHN (in Kg/mm2) of an alloy equal to 0.3 of its yield strength (in MPa) [16, 18], the slope of VHN variation versus D-1/2 can be estimated as about 0.3 of the Hall-Petch slope. Table 4 compares the Hall-Petch slopes for the alloys evaluated considering these assumptions. As can be seen here, the Hall-Petch slope of the AZ31 alloy is evaluated at 0.45 MPa.m-0.5. This number is close to similar studies on this alloy [36-37]. In addition, one can see that the Hall-Petch slopes of AZ31-1Bi and AZ31-3Bi are higher than the AZ31 ones. To explain this effect, one can see that the Hall-Petch slope is evaluated below [16]:

$$K \approx \tau c\ r0.5 \tag{2}$$

Where r is the distance of a dislocation source (i.e., Frank-Read source) from the grain boundaries and τc is the needed shear stress of this dislocation source to emit dislocations. Considering Eq. 2, one can relate the higher Hall-Petch slope of the Bi-containing alloys to the presence of fine Bi-enriched particles on the grain boundaries of AZ31-1Bi and AZ31-3Bi alloys, as mentioned above. Note that the presence of these fine particles on the grain boundaries increases the τc [17]. Therefore, the Hall-Petch slope of Bi-containing alloys is elevated. Considering these explanations, one may question

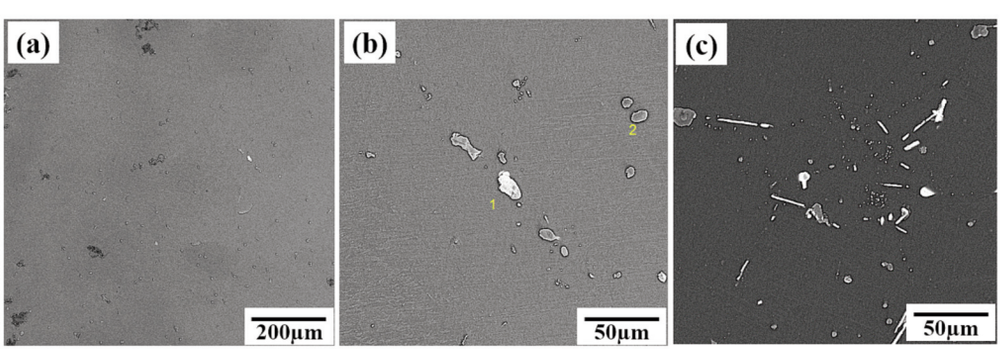

Figure 5. *FESEM microstructure of the cast alloys: (a) AZ31-0Bi, (b) AZ31-1Bi and (c) AZ31-3Bi*

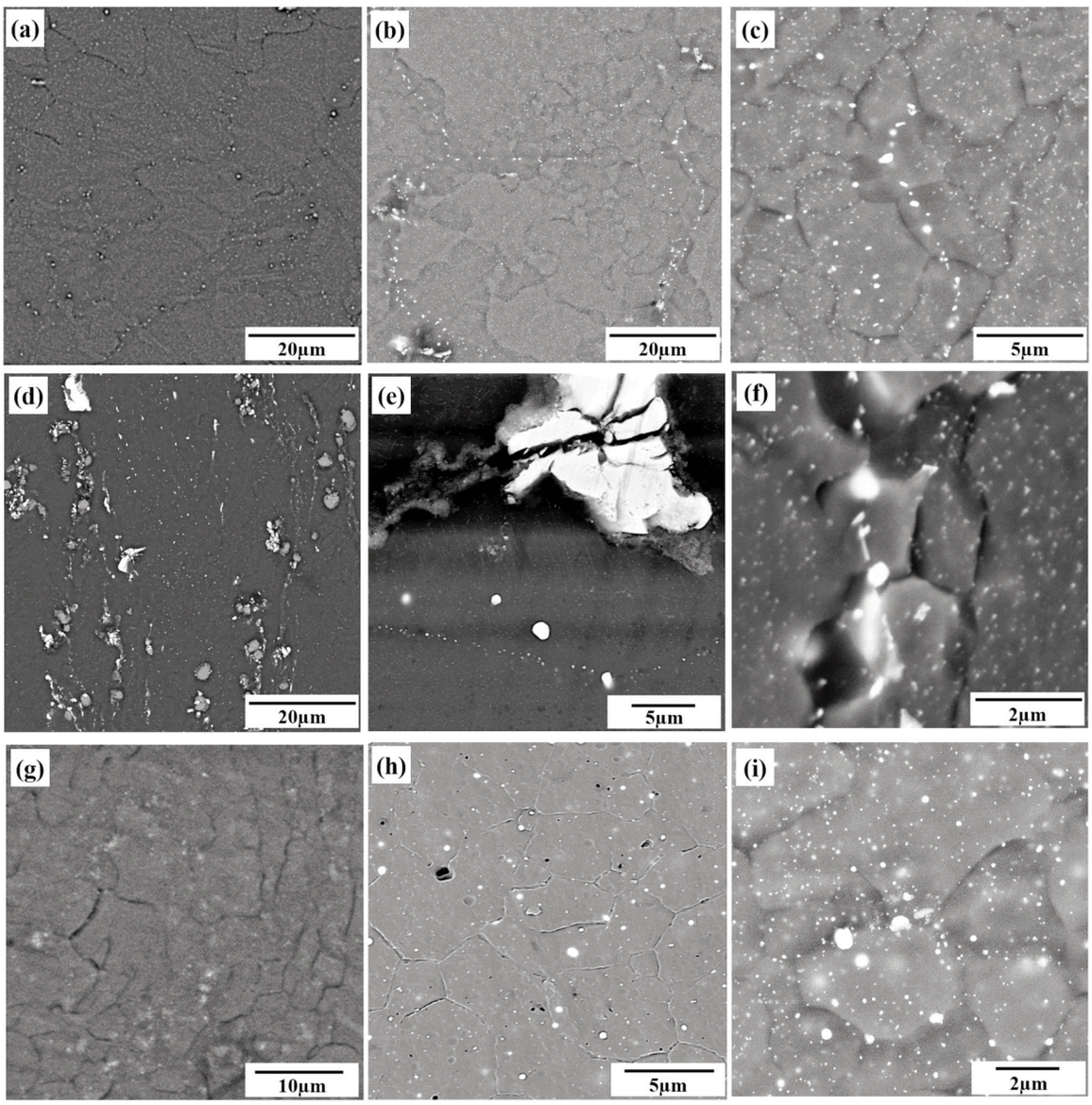

Figure 6. *FESEM microstructure of different specimens; (a) AZ31-0Bi-2, (b) and (c) AZ31-1Bi-2, (d), (e) and (f) AZ31-3Bi-2, (g) AZ31-0Bi-4, (h) AZ31-1Bi-4 and (i) AZ31-3Bi-4*

why the Hall-Petch slope of AZ31-1Bi and AZ31-3Bi are almost similar. To answer this point, it should be remembered that the Bi-enriched particles formed during casting are coarse, and these particles are only fragmented by the ECAP imposition. In addition, the second-phase particle fragmentation through SPD is saturated by the increase of volume fraction of the second-phase particles [34, 38-39]. Therefore, the number of fine particles that appeared during ECAP is limited, and this number may not significantly be increased by the increase of the Bi-content of the alloy. As a result, the effect of fine Bi-enriched particles on τc and the Hall-Petch slope is limited, and its increase by the increase of Bi-content is negligible.

Table 3. *The Vickers hardness of ECAP-processed specimens*

Alloy	Pass No.	0	1	2	4
AZ31-0Bi		48	55	70	81
AZ31-1Bi		57	85	104	107
AZ31-3Bi		63	100	123	128

Table 4. *The evaluated Hall-Petch slopes of different alloys*

Alloy	AZ31	AZ31-1Bi	AZ31-3Bi
K (MPa.m-0.5)	0.45	0.59	0.59

CC BY SA

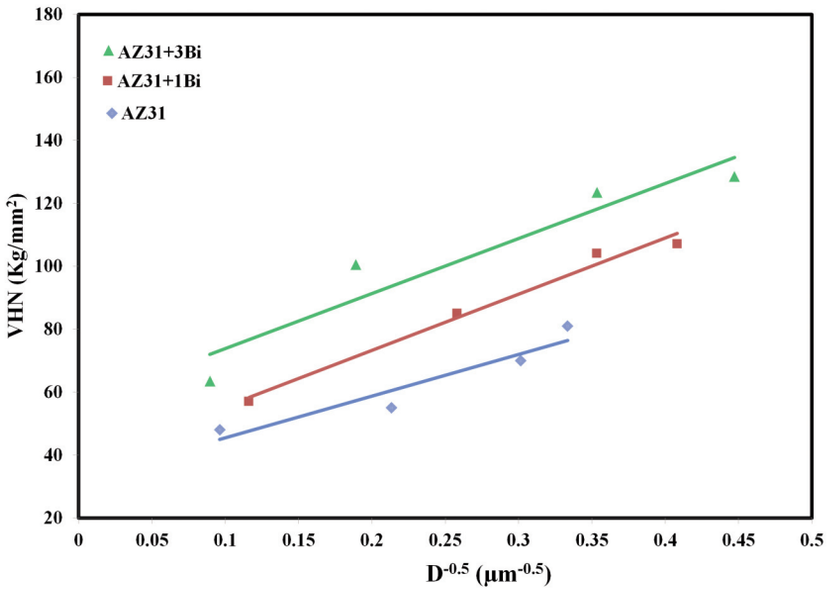

Figure 7. *The VHN of the alloys versus their inverse square root of grain size (D-0.5)*

4. Conclusions

Considering the information presented above, the effect of Bi addition on the microstructure evolution of AZ31 through severe plastic deformation can be summarized as follows:

1 - Adding Bi to the AZ31 alloy during casting leads to the formation of coarse Bi-enriched particles. The chemical composition of these particles is very close to Mg_3Bi_2.

2 - These coarse Bi-enriched particles are fragmented into fine particles through severe plastic deformation. As a result, the rate of grain refinement in the alloy increases due to the pinning effect of these fine particles on the grain boundaries.

3 - In addition to increasing the hardness of the alloy, the Hall-Petch slope also increases with Bi addition, due to the presence of fine Bi-enriched particles on the grain boundaries.

Acknowledgments

The authors thank the research board of Ferdowsi University of Mashhad (FUM) for providing research facilities and financial support through grant No. of 3/50772.

Data availability statement

Hereby, the authors declare that the research data and analysis presented in this paper are available.

Conflict of Interests

The authors the presented article approve that in publishing the presented article, they have completely followed publishing ethics, including avoiding plagiarism, transgression, data fraudulence and twofold submission. There is not any financial benefit for submitting the article and the authors has not received any financial support from a third party.

Author contribution statement

M.H. Farshidi and G.R. Ebrahimi contributed to the study conception and design. Material preparation, data collection and analysis were performed by J. Yazdi and M.H. Farshidi. The first draft of the manuscript was written by M.H. Farshidi. All authors have read and approved the final manuscript.

References

[1] Z. Zhang, A. Couture, An investigation of the properties of Mg-Zn-Al alloys, Scripta Materialia, 39 (1) (1998) 45-53. https://doi.org/10.1016/S1359-6462(98)00122-5

[2] S.V. Satya Prasad, S.B. Prasad, K. Verma, R.K. Mishra RK, V. Kumar, S. Singh, The role and significance of magnesium in modern day research-a review, Journal of Magnesium Alloys, 10 (2022) 1–61. https://doi.org/10.1016/j.jma.2021.05.012

[3] Y. Kawamura Y, S. Yoshimoto, M. Yamasaki, Microstructure and mechanical properties of extruded Mg-Zn-Y alloys with 14H long period ordered structure, Materials Transaction, 47 (4) (2006) 959-965. https://doi.org/10.2320/matertrans.47.959

[4] R. Radha, D. Sreekanth, Insight of magnesium alloys and composites for orthopedic implant applications –a review, Journal of Magnesium Alloys, 5 (3) (2017) 286–312. https://doi.org/doi: 10.1016/j.jma.2017.08.003

[5] W. Ya-Xiao, Z. Ji-Xue, W. Jie, L. Tian-Jiao, Y. Yuan-Sheng, Effect of Bi addition on microstructures and mechanical properties of AZ80 magnesium alloy, Transaction of Nonferrous Metals Society of China, 21 (2011) 711-716. https://doi.org/10.1016/S1003-6326(11)60770-X

[6] Y. Guangyin, S. Yangshan, D. Wenjiang, Effects of bismuth and antimony additions on the microstructure and mechanical properties of AZ91 magnesium alloy, Materials Science and Engineering A, 308 (2001) 38-44. https://doi.org/10.1016/S0921-5093(00)02043-8

[7] H. Moshver, M. Haddad-Sabzevar, M. Mazinani, M. Mahmoudi, Effect of bismuth on microstructure, mechanical properties and fracture behavior of AZ magnesium alloys, Materials Science and Engineering A, 854 (2022) 143676. https://doi.org/10.1016/j.msea.2022.14367

[8] H. Xue, X. Li, W. Zhang, Z. Xing Z, J. Rao, F.S. Pan, Effect of Bi on microstructure and mechanical properties of extruded AZ80-2Sn magnesium alloy, High Temperature Materials Processing, 37 (1) (2018) 97-103. https://doi.org/10.1515/htmp-2016-0045

[9] Superior room temperature ductility of magnesium dilute binary alloy via grain boundary sliding, Scripta Materialia, 150 (2018) 26-30. https://doi.org/10.1016/j.scriptamat.2018.02.034

[10] H. Somekawa, A. Singh, R. Sahara, T. Inoue, Excellent room temperature deformability in high strain rate regimes of magnesium alloy, Scientific Reports, 8 (2018) 656. https://doi.org/10.1038/s41598-017-19124-w

[11] C. Niu, C. Li C, Assessment of the Al-Bi-Mg system and extrapolation to the Al-Bi-Mg-Sn quaternary system, Calphad, 60 (2018) 37-49. https://doi.org/10.1016/j.calphad.2017.11.003

[12] N. Ono, R. Nowak, S. Miura, Effect of deformation temperature on Hall–Petch relationship registered for polycrystalline magnesium, Material Letters, 58 (1-2) (2004) 39-43. https://doi.org/10.1016/S0167-577X(03)00410-5

[13] S.M. Razavi, D.C. Foley, I. Karaman, K.T. Hartwig, O. Duygulu, L.J. Kecskes, S.N. Mathaudhud, V.H. Hammond, Effect of grain size on prismatic slip in Mg–3Al–1Zn alloy, Scripta Materialia, 67 (2012) 439–442. http://dx.doi.org/10.1016/j.scriptamat.2012.05.017

[14] Z.C. Cordero, B.E. Knight, C.A. Schuh, Six decades of the Hall-Petch effect- a survey of grain-size strengthening studies on pure metals, International Materials Review, 61 (8) (2016) 495-512. https://doi.org/10.1080/09506608.2016.1191

[15] C.H. Cacers, G.E. Mann GE, J.R. Griffiths JR, Grain size hardening in Mg and Mg-Zn solid solutions, Metallurgical and Materials Transaction A, 42 (2011) 1950-1959. https://doi.org/10.1007/s11661-010-0599-2

[16] D. Zhou, H. Wang, D.W. Saxey, O. Muransky, H. Geng, W.D.A. Rickard, Z. Quadir, C. Yang, S.M. Reddy, D. Zhang D, Hall–Petch slope in ultrafine grained Al-Mg Alloys, Metallurgical and Materials Transaction A, 50 (2019) 4047-4057. https://doi.org/10.1007/s11661-019-05329-3

[17] S. Ren, Z. Sun, Z. Xu, R. Xin, J. Yao, D. Lv, J. Chang, Effects of twins and precipitates at twin boundaries on Hall–Petch relation in high nitrogen stainless steel, Journal of Materials Research, 33 (2018) 1764-1772. https://doi.org/10.1557/jmr.2018.138

[18] Y.S. Sato, M. Urata, H. Kokawa, K. Ikeda K, Hall Petch relationship in friction stir welds of equal channel angular-pressed aluminium alloys, Materials Science and Engineering A, 354 (2003) 298-305. https://doi.org/10.1016/S0921-5093(03)00008-X

[19] T. Sakai, A. Belyakov, R. Kaibyshev, H. Miura, J.J. Jonas, Dynamic and post-dynamic recrystallization under hot, cold and severe plastic deformation conditions, Progress in Materials Science, 60 (2014) 130-207. https://doi.org/10.1016/j.pmatsci.2013.09.002

[20] Y. Estrin, A. Vinogradov, Extreme grain refinement by severe plastic deformation: a wealth of challenging science, Acta Materialia, 61 (2013) 782-817. https://doi.org/10.1016/j.actamat.2012.10.038

[21] Y. Estrin, A. Vinogradov, Analytical and numerical approaches to modelling severe plastic deformation, Progress in Materials Science, 95 (2018) 172-242. https://doi.org/10.1016/j.pmatsci.2018.02.001

[22] V.M. Segal, Materials processing by simple shear, Materials Science and Engineering A, 197 (1995) 157-164. https://doi.org/10.1016/0921-5093(95)09705-8

[23] V.M. Segal, Equal channel angular extrusion of flat products, Materials Science and Engineering A, 476 (2008) 178-185. https://doi.org/10.1016/j.msea.2007.04.092

[24] Y.C. Yuan, A.B. Ma, J.H. Jiang, Y. Sun, F.M. Lu, L.Y. Zhang, D. Song, Mechanical properties and precipitate behavior of Mg–9Al–1Zn alloy processed by equal-channel angular pressing and aging, Journal of Alloys and Compounds, 594 (2014) 182–188. https://doi.org/10.1016/j.jallcom.2014.01.140

[25] S.M. Arab, A. Akbarzadeh, The effect of equal channel angular pressing process on the microstructure of AZ31 Mg alloy strip shaped specimens, Journal of Magnesium Alloys, 1 (2013) 145-149. http://dx.doi.org/10.1016/j.jma.2013.07.001

[26] J. Li, W. Xu, X. Wu, H. Ding H, K. Xia K, Effects of grain size on compressive behaviour in ultrafine grained pure Mg processed by equal channel angular pressing at room temperature, Materials Science and Engineering A, 528 (2011) 5993-5998. https://doi.org/10.1016/j.msea.2011.04.045

[27] X. Yu, Y. Li, Q. Wei, Y. Guo, T. Suo, F. Zhao, Microstructure and mechanical behavior of ECAP processed AZ31B over a wide range of loading rates under compression and tension, Mech Mater 86 (2015) 55-70. https://doi.org/10.1016/j.mechmat.2015.03.001

[28] S.X. Ding, W.T. Lee, C.P. Chan, L.W. Chang, P.W. Kao, Improvement of strength of magnesium alloy processed by equal channel angular extrusion, Scripta Materialia, 59 (2008) 1006-1009. https://doi.org/10.1016/j.scriptamat.2008.07.007

[29] A. Muralidhar, S. Narendranath, H.S. Nayaka, Effect of equal channel angular pressing on AZ31 wrought magnesium alloys, Journal of Magnesium Alloys, 1 (2013) 336-340. https://doi.org/10.1016/j.jma.2013.11.007

[30] H. Mirzadeh, Grain refinement of magnesium alloys by dynamic recrystallization (DRX): A review, Journal of

Materials Research and Technology, 25 (2023) 7050-7077. https://doi.org/10.1016/j.jmrt.2023.07.150

[31] J. Bahadori-Fallah, M.H. Farshidi, A.R. Kiani-Rashid, Equal channel angular pressing of spheroidal graphite cast iron, Materials Research Express, 6 (2019) 066542. https://doi.org/10.1088/2053-1591/ab0dcf

[32] F. Dong, Y. Yi, C. Huang, S. Huang, Influence of cryogenic deformation on second-phase particles, grain structure, and mechanical properties of Al-Cu-Mn alloy, Journal of Alloys and Compounds, 827 (2020) 154300. https://doi.org/10.1016/j.jallcom.2020.154300

[33] I. Gutierrez-Urrutia, M.A. Munoz-Morris, D.G. Morris, Contribution of microstructural parameters to strengthening in an ultrafine-grained Al–7% Si alloy processed by severe deformation, Acta Materialia, 55 (2007) 1319-1330. https://doi.org/10.1016/j.actamat.2006.09.037

[34] B.B. Straumal, R. Kulagin, L. Klinger, E. Rabkin, P.B. Straumal, O.A. Kogtenkova, B. Baretzky, Structure refinement and fragmentation of precipitates under severe plastic deformation: a review, Materials, 15 (2) (2022) 601. https://doi.org/10.3390/ma15020601

[35] H.A. Carmona, A.V. Guimaraes, J.S. Andrade, I. Nikolakopoulos, F.K. Wittel, H.J. Herrmann, Fragmentation processes in two-phase materials, Physical Review, E91 (2015) 012402. https://doi.org/10.1103/PhysRevE.91.012402

[36] H. Yu, Y. Xin, M. Wang, Q. Liu, Hall-Petch relationship in Mg alloys: A review, Journal of Materials Science and Technology, 34 (2) (2018) 248-256. https://doi.org/10.1016/j.jmst.2017.07.022

[37] G. Garces, A. Clemente, J. Medina, P. Perez, A. Stark, N. Schell, P. Adeva, Temperature dependence of Hall–Petch parameters using in situ diffraction experiments in AZ31 alloy, JOM, 74 (7) (2022) 2622-2634. https://doi.org/10.1007/s11837-022-05320-1

[38] J.M. Cubero-Sesin, Z. Horita, Strengthening of Al through addition of Fe and by processing with high-pressure torsion, Journal of Materials Science, 48 (2013) 4713-4722. https://doi.org/10.1007/s10853-012-6935-8

[39] D.G. Morris, M.A. Muñoz-Morris, Refinement of second phase dispersions in iron aluminide intermetallics by high-temperature severe plastic deformation, Intermetallics, 23 (2012) 169-176. https://doi.org/10.1016/j.intermet.2011.11.020

MIKROSTRUKTURA I TVRDOĆA LEGURA MAGNEZIJUMA AZ31 MODIFIKOVANIH BIZMUTOM PODVRGNUTIH INTENZIVNOJ PLASTIČNOJ DEFORMACIJI

J. Yazdi, M.H. Farshidi *, G.-R. Ebrahimi

Katedra za nauku o materijalima i inženjerstvo, Fakultet za inženjerstvo, Univerzitet Ferdousi u Mašhadu, Trg Azadi, Mašhad, Iran

Apstrakt

Legure magnezijuma su poznate kao atraktivni materijali zbog svoje niske gustine i dobre toplotne provodljivosti. Međutim, u poređenju sa konkurentnim metalnim materijalima kao što su legure aluminijuma, legure magnezijuma imaju manju čvrstoću. Među različitim metodama uvedenim za ojačavanje metalnih materijala, intenzivna plastična deformacija je značajna zbog svoje efikasnosti i relativne jednostavnosti. Ova studija istražuje uticaj sadržaja bizmuta na evoluciju mikrostrukture i tvrdoću legure magnezijuma AZ31 podvrgnute intenzivnoj plastičnoj deformaciji presovanjem kroz kanal pod jednakim uglom (engl. equal channel angular pressing - ECAP). Za ovu svrhu, legure AZ31 sa nominalnim sadržajem bizmuta od 0%, 1% i 3% su obrađivane do četiri prolaza presovanja kroz kanal pod jednakim uglom na 300 °C. Evolucija mikrostrukture ovih legura je zatim ispitana korišćenjem optičke i skenirajuće elektronske mikroskopije. Tvrdoća uzoraka je merena korišćenjem Vikersove metode. Rezultati pokazuju da su čestice druge faze obogaćene bizmutom fragmentisane tokom intenzivne plastične deformacije. Pored toga, povećanje sadržaja bizmuta dovodi do bržeg usitnjavanja zrna tokom intenzivne plastične deformacije usled efekta pinovanja (zadržavanja) ovih čestica druge faze na granicama zrna. Veći stepeni ojačavanja tokom intenzivne plastične deformacije su primećeni za legure AZ31 koje sadrže bizmut. Ovaj efekat se pripisuje bržem usitnjavanju zrna i povećanju Hol-Pečovog (engl. Hall-Petch) koeficijenta koji proističe iz prisustva finih čestica obogaćenih bizmutom.

Ključne reči: *Legura magnezijuma AZ31; Dodatak bizmuta; Intenzivna plastična deformacija; Usitnjavanje zrna; Tvrdoća*